



Polyamine-functionalized carbon dots as active catalyst for Knoevenagel condensation reactions

Faezeh Farzaneh¹ · Soodabeh Aghabali¹ · Zahra Azarkamanzad¹

Received: 4 May 2020 / Accepted: 9 July 2020 / Published online: 14 July 2020
© Akadémiai Kiadó, Budapest, Hungary 2020

Abstract

In this study, carbon dots coated with diluted polyethylene imine was prepared from the carbonization of citric acid (CA) with branched polyethylene imine (BPEI) at temperature (200 °C), designated as BPEI-CDs. The solid catalyst was characterized by various techniques including X-ray powder diffraction (XRD), Fourier transform infrared (FT-IR), atomic force microscopy (AFM), high resolution transmission electron microscopy (HRTEM). The obtained BPEI-CDs are spherical graphite nanocrystals (averaging 5–10 nm). It was found that it could be used as heterogeneous catalyst for Knoevenagel condensation of aromatic aldehydes with malononitrile at 60 °C in ethanol. The Knoevenagel aromatic products were obtained with a moderate to excellent conversion within 2 h. The BPEI-CDs as catalyst was easily isolated from the reaction mixtures by simple filtration and reused for three times without significant loss of catalytic activity. There was also no contribution from the leached active species and conversion was only being possible in the presence of the prepared modified carbon dots.

Keywords Carbon dots · Knoevenagel condensation · Branched polyethylene imine · Citric acid

Introduction

The ability of carbon atoms to form covalent bonds with other atoms via sp , sp^2 and sp^3 enables it to form different allotropies such as, diamond, graphite, carbon nanotube, carbon dots and so on [1]. Carbon-based quantum dots with fascinating

Electronic supplementary material The online version of this article (<https://doi.org/10.1007/s11144-020-01826-4>) contains supplementary material, which is available to authorized users.

✉ Faezeh Farzaneh
farzaneh@alzahra.ac.ir; faezeh_farzaneh@yahoo.com

¹ Department of Chemistry, Faculty of Physics & Chemistry, Alzahra University, P.O. Box 1993891176, Vanak, Tehran, Iran

properties such as great potential applications in bioimaging, optoelectronics sensors, SERS, and photocatalyst have gradually become a rising star as a new nano-carbon member due to their benign, abundant and inexpensive nature [2–4]. A great variety of techniques and methods have been developed in recent years for preparation of C-dots such as chemical ablation [5–7], electrochemical carbonization [8–11], laser ablation [12], microwave irradiation [13] solvothermal and hydrothermal methods [14] are provided. On the other hand, other methods such as thermal decomposition of organic compounds in solvent with high boiling points is a simple and inexpensive procedure for preparing C-dots. This method is based on heating nitrogen- and oxygen rich organic molecules in an autoclave above 200 °C. Zhang et al. have reported N-doped C-dots can be formed by heating toluene solution of CCl_4 and NaNH_2 [15]. Other methods have also been used for preparation C-dots such as thermal decomposition [16, 17] and ultrasonic carbonization [18].

Recently a single step method based on thermal decomposition of substituted ammonium citrate salts are reported. Based on reported citric acid is one of the starting materials as carbon source in which solutions of branched poly(ethyleneimine) (BPEI) in water at 200 °C causes formation of C-dots modified with (BPEI) [16].

In this study, attempts have been made to use this type of C-dots as catalyst for Knoevenagel reactions because of basic character of C-dots surfaces.

The Knoevenagel reaction is due to the carbon–carbon bond formation between active methylene group and aldehydes or ketones. The Knoevenagel products have been widely used for the preparation of coumarin derivatives, cosmetics, perfumes, pharmaceutical compounds, polymers and so on [19–21]. Up to now various Lewis acids and bases have conventionally been used as homogeneous catalyst [22–26]. Because of separation and recyclability problems of homogeneous catalyst, many efforts have been made to use heterogeneous system such as molecular sieves [27] organic functionalized molecular sieves, or silica [28–30] metal organic frameworks (MOF) such as UiO-66 [31], Zif-8 [32], Zif-9 [33], IRMOF [34], and mixed oxides nanoparticles [35] are active for Knoevenagel reactions.

Experimental

All chemicals were purchased from Merck Chemical Company, and used without further purification. XRD patterns of powdered samples were carried out on Siefert 3003 PTS diffractometer using Cu K_α radiation ($k = 1.5406 \text{ \AA}$) in the 2θ range of 10° to 60° with accelerating voltage and current of 40 kV and 40 mA, respectively. FT-IR spectra were recorded on a Bruker instrument using KBr pellets technique in the range of $4000\text{--}500 \text{ cm}^{-1}$. The Atomic Force Microscopy (AFM) images were taken by Nanosurf easyscan 2. The products were analyzed by gas chromatography (GC) (Agilent Technologies, 6890 Series GC System, HP-5 Phenyl Methyl Siloxane Capillary, $30 \text{ m} \times 530 \mu\text{m} \times 1.5 \mu\text{m}$ Nominal, Carrier Gas; He) GC–MS analyses were performed using an 5973 Network Mass Selective Detector, 6890 Network, GC System, Column; HP Phenyl Methyl Siloxane Capillary, $30 \text{ m} \times 530 \mu\text{m} \times 1.5 \mu\text{m}$ Nominal, Carrier Gas; He. High Resolution Transmission Electron Microscopy (HRTEM) were performed using a Tecnai, FEI.

Preparation BPEI-CDs as catalyst

BPEI-CDs was prepared as reported [16–18]. CDs with BPEI coatings are produced by a mixture of citric acid (CA) with branched polyethylene imine (BPEI) at temperature (200 °C). Therefore 0.5 g of BPEI and 1 g of CA are dissolved uniformly with 10 mL of hot water in a 25 mL beaker, and then heated moderately (< 200 °C) using a heating mantle. Most of water evaporated for about 20 min, until a uniform pale-yellow gel was formed. Then one 1 mL of water was added before the gel was scorched and heating was continued. This procedure was repeated about 10 times (in 3 h), then the gel with orange color was obtained. The product was used without further purification. In this step, carbon dots with polyethyleneimine was obtained.

Catalyst test

In a typical experiment BPEI-CDs (25 mg), malononitrile (5 mmol), aldehyde (5 mmol) and solvent as ethanol (1.5 mL) were placed into round bottom flask (25 mL) and the reaction mixture was stirred at 60 °C for 2 h. Then the mixture was dissolved in 2 mL ethyl acetate and the Knoevenagel products were separated and subjected to GC and GC–MS analysis. The catalyst was recovered by simple filtration, washing with ethanol and drying in air in order to use in the next run.

Result and discussion

Catalyst characterization

In this study, BPEI-CDs was prepared based on reported [16], with citric acid and branched polyethylene imine.

The XRD pattern of BPEI-CDs is shown in Fig. 1, the obtained results is consistent with those reported before [16]. The typical diffractions at $2\theta = 21.68^\circ$ and 43° are related to the (002) and (100) planes respectively. In fact, the obtained results of BPEI-CD indicates the presence of carbon-based materials and graphite crystalline plates [16, 36].

The FT-IR spectra of citric acid, BPEI and BPEI-CD are shown in Fig. 2a–c respectively. The obtained results were consistent with those reported before [16]. The FT-IR spectrum of the BPEI-CDs is similar to that of the BPEI (3440 and 1585 cm^{-1} due to NH CH_2 at 2950 and 2820 cm^{-1} and CN at 1338 cm^{-1}), but no characteristic absorption of CA was observed. These results indicate that CA might be mostly carbonized during the pyrolysis, while the BPEI kept stable. In fact, observing a peak at 1700 cm^{-1} in Fig. 2c should be attributed to the $-\text{CONH}$ stretching vibrations.

The AFM images of BPEI-CDs are shown in Fig. 3 the particle size distribution of BPEI-CD is 5 to 50 nm. Most particles have a size of 5 to 10 nm.

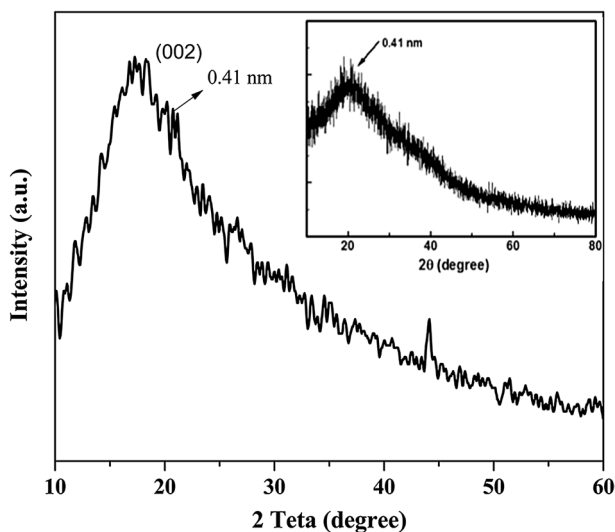


Fig. 1 The XRD pattern of BPEI-CDs

The HRTEM with two different magnification of modified C-dots are shown in Fig. 4. HRTEM images (Figs. 4a and 4b) reveals that BPEI-CDs spherical morphology with average particle size of 5–10 nm, but the majority of particle sizes are 5 nm. Based on the SAED results, the spacing between the crystalline lattice is around 0.26 nm.

The EDX of CDs is shown in Fig. 5, which indicates the presence of carbon, nitrogen and oxygen in the prepared BPEI-CDs.

Catalytic activity

Optimization of the Knoevenagel condensation reaction

The Knoevenagel condensation reaction of benzaldehyde with malononitrile was performed in the presence of BPEI-CD as catalyst to form benzylidene malononitrile (Scheme 1).

Various parameters such as the effect of catalyst amount, temperature, reaction time and solvent were evaluated. At first, to optimize the catalyst amount, reaction was carried out using 5, 13, 17 and 25 mg of BPEI-CD as catalyst within 2 h, in refluxing ethanol (Fig. 6). As seen in this figure, whereas increasing the amount of catalyst from 5 to 25 mg within 2 h increases the conversion from 87 to 100% with 72 to 100% selectivity toward the benzylidene malononitrile (Fig. 6).

Then, the effects of reaction temperature on catalytic activity were investigated (Fig. 7). The results showed that the reaction conversion gradually increased from 30 °C to 50 °C, but the maximum conversion (100%) of the product was obtained at 60 °C within 2 h.

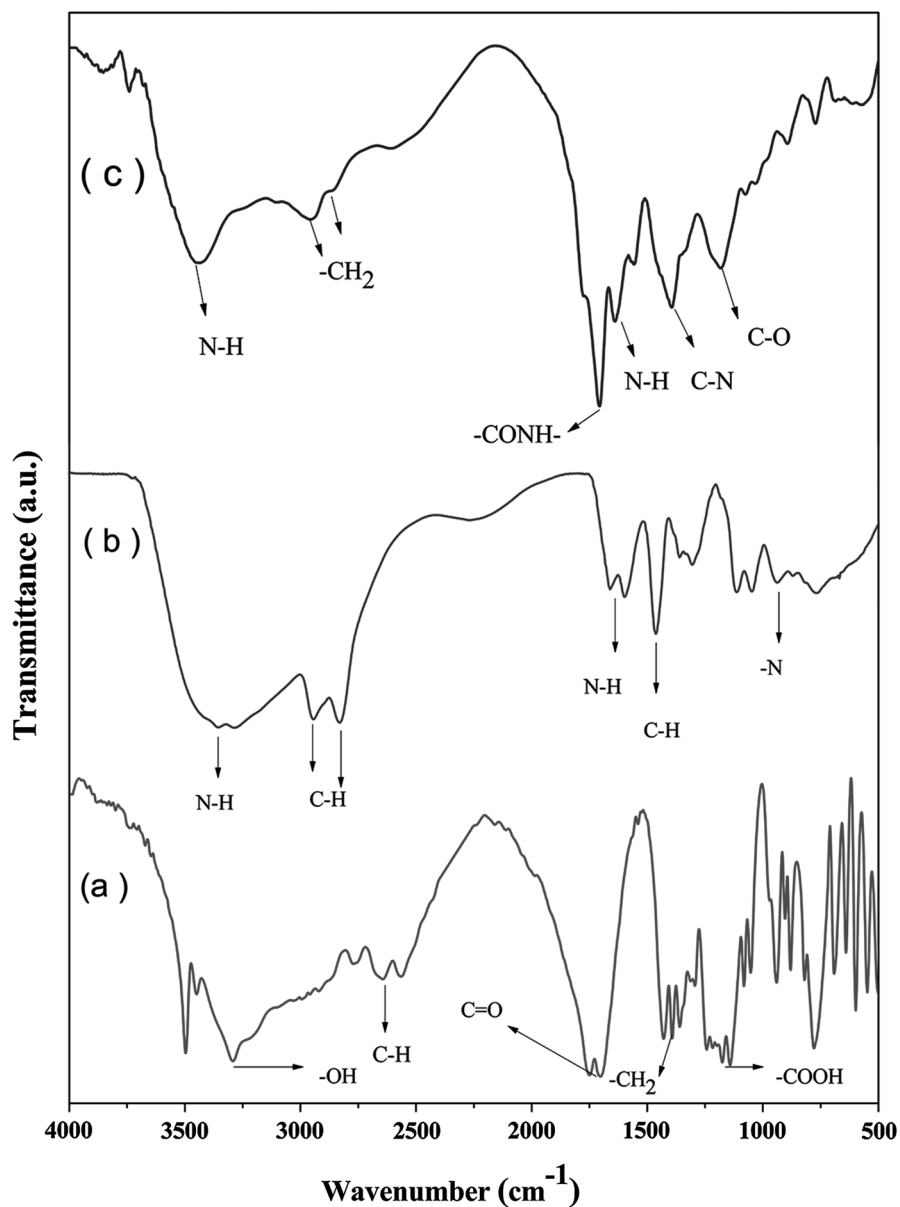
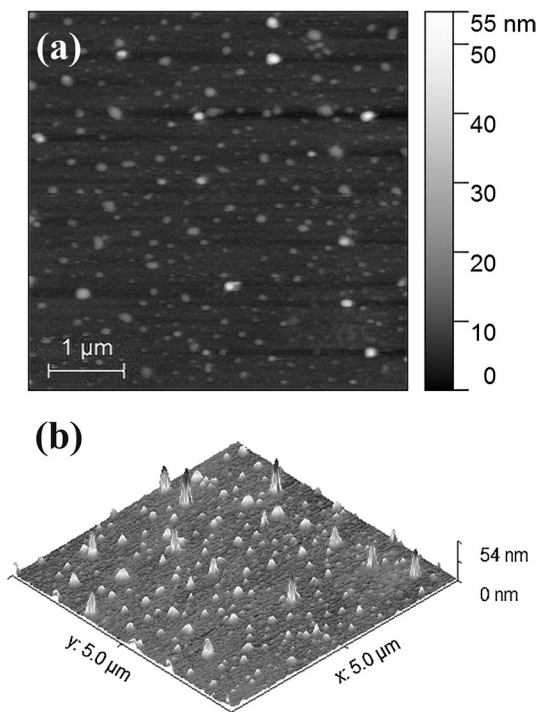


Fig. 2 FT-IR spectra of (a) citric acid, (b) BPEI, (c) BPEI-CDs

In order to evaluate the effect of time on the Knoevenagel reaction, the reaction was performed at 60 °C for different reaction times from 30 min to 2 h (Fig. 8). With increasing reaction time, the conversion of benzaldehyde increased to 100% after 2 h. Therefore, all other reactions were carried out within 2 h.

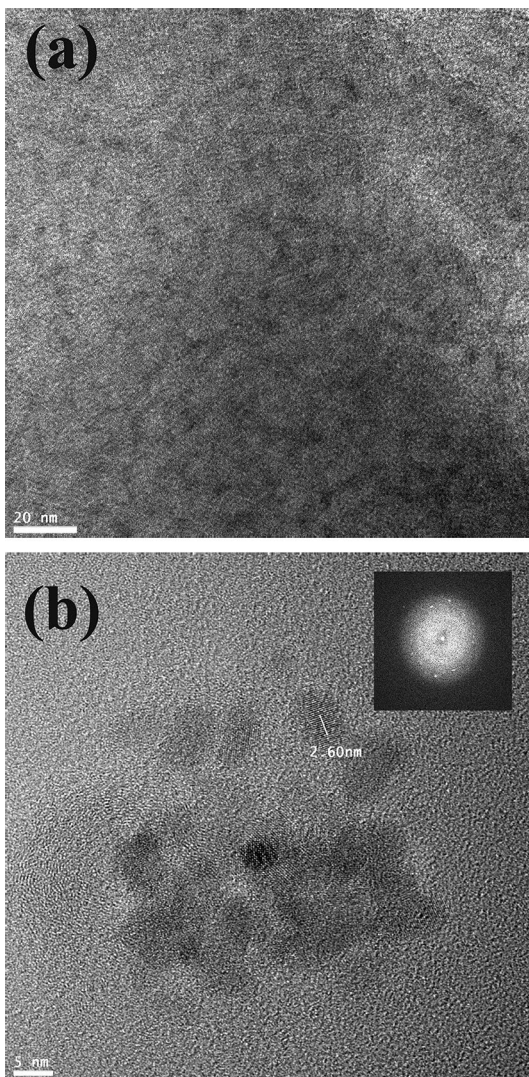
Fig. 3 AFM image of BPEI-CDs with two maps



In order to investigate the effect of solvent on the product formation, reactions were carried out with different solvents such as methanol, ethanol, butanol, DMF and toluene (Fig. 9). It was found that the highest and lowest catalytic activity is observed in ethanol and toluene, respectively. As such, it can be concluded that the less polar solvents such as toluene are not suitable media for this reaction. In contrast, ethanol as a rather polar and eco-friendly solvent is better perhaps due to the stabilization of the generated partial ionic transition state structure. In fact, the reactivity of the catalyzed reactions to solvent depends on the (a) polarity and amphiprotic properties of catalyst surface [32, 33, 37]. For example, whereas some reactions in the presence of MOF catalyst such as UiO-66-NH₂ exhibits the highest catalytic activity in DMF, ethanol is a good media as well. On the other hand, ethanol was found to be better than DMF in cases such IRMOF-3 [37] and NH₂-MIL(AI) [32] catalysts. This may be due to the amphiprotic character of solid surfaces [34]. It was also reported that toluene is better than polar solvents for some amino-tagged silicas [33, 38]. In contrast, the polar solvent increases the reaction rate in some other Knoevenagel catalyzed reactions. Therefore, there is no general trend in the effect of solvent on Knoevenagel reactions using heterogeneous catalysis system.

Having established the optimal reaction conditions, we examined the generality of this Knoevenagel condensation on other substrates such as 3-nitrobenzaldehyde, 2-chlorobenzaldehyde, 4-chlorobenzaldehyde, 2-hydroxybenzaldehyde, 4-hydroxybenzaldehyde, 4-methylbenzaldehyde, 4-methoxybenzaldehyde and furfural in ethanol (1.5 mL) using 0.025 g of catalyst within 2 h, at 60 °C (Table 1).

Fig. 4 HRTM image of BPEI-CDs with two magnifications



Effect of the substitution on the conversion percentages can be rationalized if one has an insight into the reaction mechanism. As indicated in Scheme 2, it seems likely that the BPEI-CDS as Lewis base (LB) abstracts a H^+ from malononitrile and generates compound **A**. Subsequently, **A** reacts with aldehyde to afford **B**. Protonation followed by elimination of water results in the formation of **C** and Knoevenagel adduct **D**, respectively. Effect of the substitutions on the conversion rate supports the suggested mechanism. As seen in the Scheme 2, the presence of electron-withdrawing group in meta or para position of aldehyde should accelerate the reaction rate due to the stabilization of the intermediate **B**. This in turn increases the conversion rate (entries 1, 2 and 4, Table 1). On the other hand, the presence of electron-donating

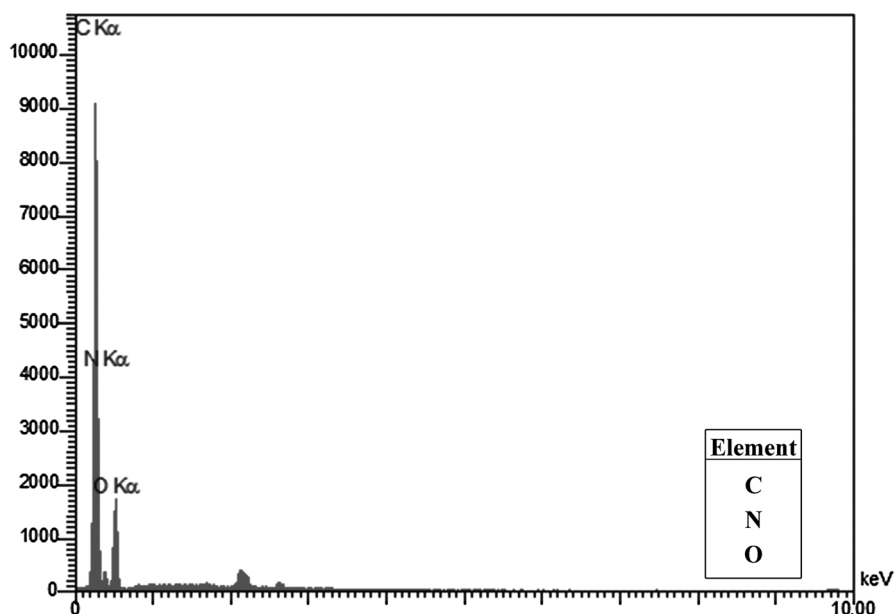
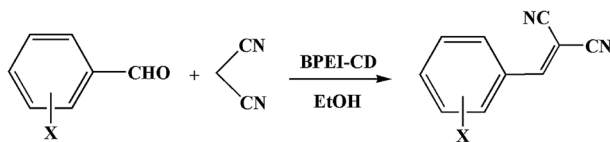


Fig. 5 The EDX of BPEI-CDs



Scheme 1 The Knoevenagel condensation reaction of benzaldehyde derivatives with malononitrile

groups on para position retards the conversion rate due to the destabilization of the intermediate **B**. This in turn gives the corresponding product in lower yield (entries 6, 7 and 8, Table 1). That ortho-chloroaldehyde has afforded the product in lower yield (entry 3, Table 1) may have been the result of partial steric effect experienced between the rather large chlorine atom and reaction center. Finally, observation of excellent yield in the case of ortho-hydroxy aldehyde (entry 5, Table 1) is not surprising since the formation of hydrogen bonding between the $-OH$ group and $-C=O$ in the transition state increases the conversion rate (inset, Scheme 2, **E**).

The recyclability of BPEI-CDs was investigated under optimum reaction conditions. After each reaction run the catalyst was recovered by centrifugation, washed with ethanol for several times and dried under vacuum at $100\text{ }^{\circ}\text{C}$. As shown in Fig. 10, the catalyst maintains with high catalytic activity (100% conversion and 100% selectivity), after three recycling step a very slight decreasing was observed (with 99% conversion and 98% selectivity). On the other hand, no catalytic activity was observed using the filtrate solution. The obtained results indicate the heterogeneous character of the prepared catalyst.

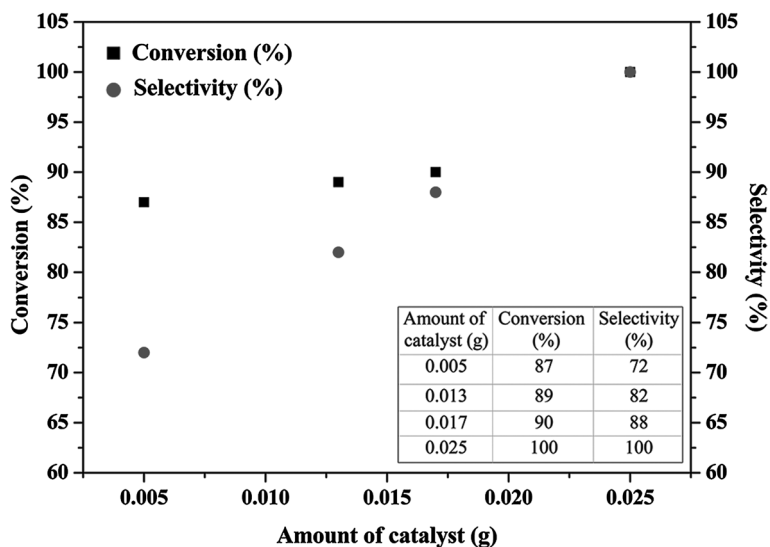


Fig. 6 Influence of catalyst amount on Knoevenagel condensation. Reaction conditions: benzaldehyde (5 mmol), malononitrile (5 mmol), solvent: ethanol (1.5 ml), 60 °C, 2 h

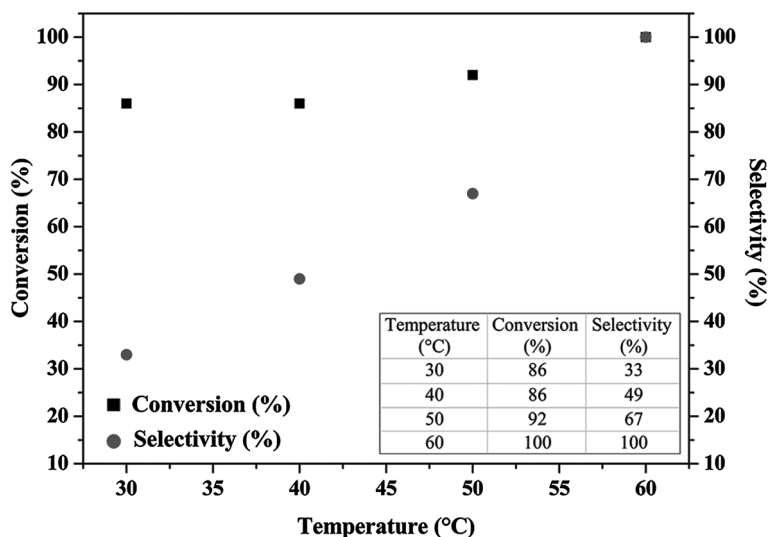


Fig. 7 Influence of reaction temperature on Knoevenagel condensation. Reaction conditions: benzaldehyde (5 mmol), malononitrile (5 mmol), solvent: ethanol (1.5 ml), catalyst 0.025 g, 2 h

The other point is the FT-IR spectra before and after experiment were similar (Fig. 11).

The XRD patterns of BPEI-CDs before and after reaction is shown in Fig. S1. The intensity of broad diffraction peak at $2\theta = 24.0$ (d_{002}) was decreased and the

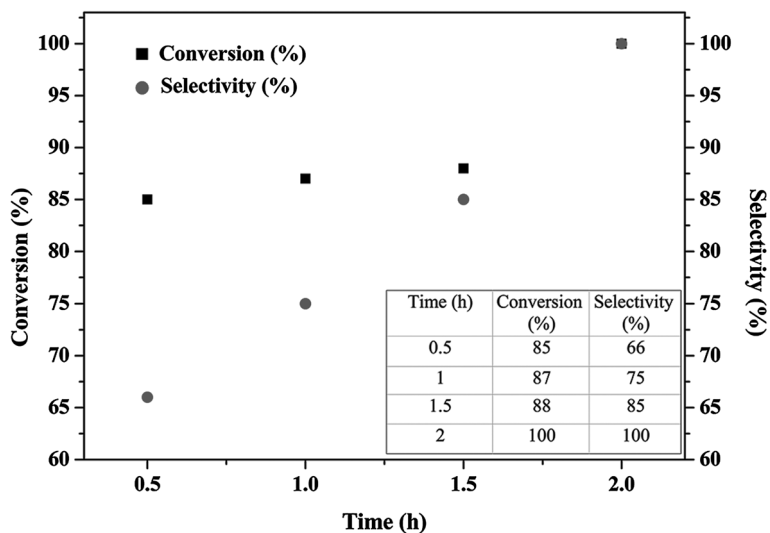


Fig. 8 Influence of reaction time on Knoevenagel condensation. Reaction conditions: benzaldehyde (5 mmol), malononitrile (5 mmol), solvent: ethanol (1.5 ml), catalyst 0.025 g, 60 °C

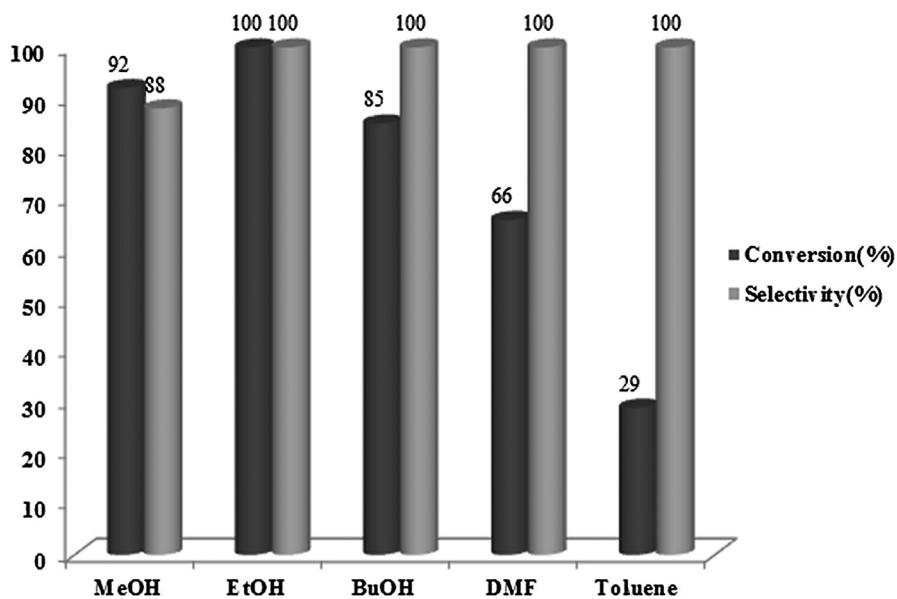


Fig. 9 The effect of solvent on product formation reaction conditions: aldehyde (5 mmol), malononitrile (5 mmol), catalyst 0.025 g, 60 °C, 2 h

Table 1 Results obtained for Knoevenagel condensation of aldehydes

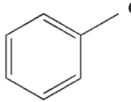
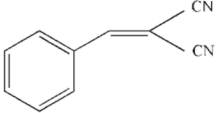
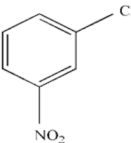
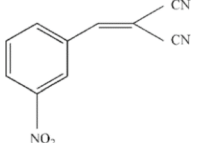
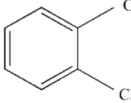
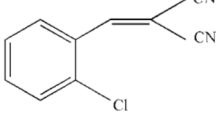
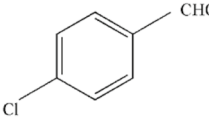
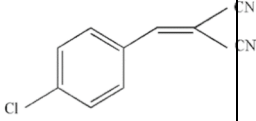
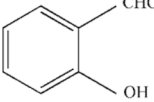
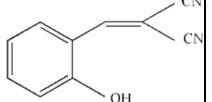
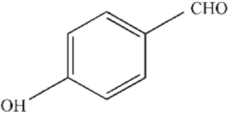
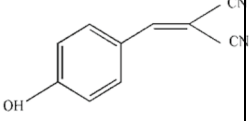
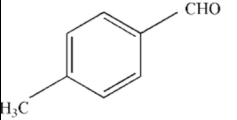
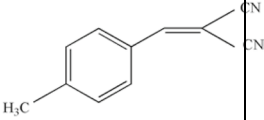
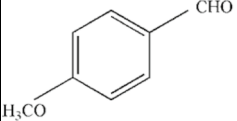
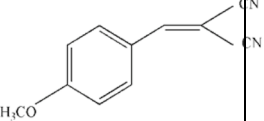
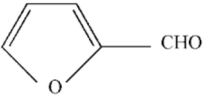
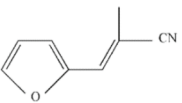
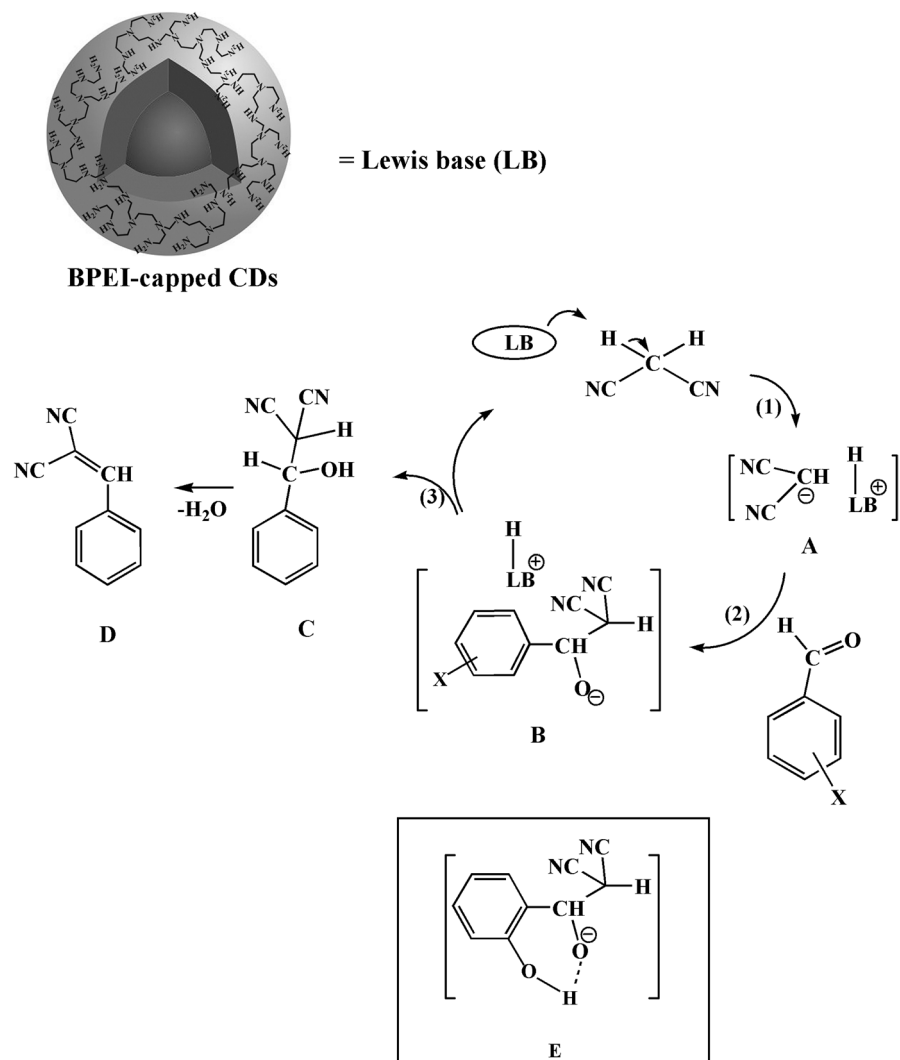
Entry	Aldehyde	Product	Conversion ^a (%)	Selectivity (%)
1			100	100
2			100	100
3			90	90
4			100	100
5			100	100
6			65	100
7			84	77
8			68	83
9			90	68

Table 1 (continued)

Reaction conditions: aldehydes (5 mmol), malononitrile (5 mmol), solvent: ethanol (1.5 mL), catalyst 0.025 g, 60 °C, 2 h



Scheme 2 Suggested mechanism for catalyzed Knoevenagel condensation reaction of aldehydes with malononitril. Inset, the stabilized intermediate **E** due to the formation of intramolecular hydrogen bond

intensity of weak peak at 43.4 (d100) has been increased. These results indicate the amorphous carbon phase decreased and graphitic phase increased which are consistent with those reported before [36]. The interesting point is the XRD pattern of BPEI-CDs after second and third run were similar.

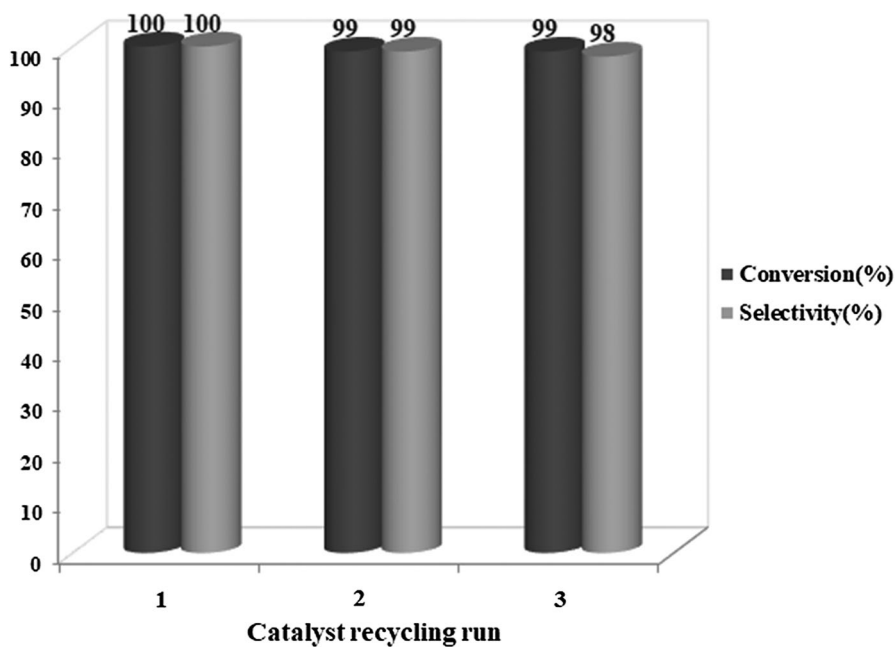


Fig. 10 The effect of recyclability of catalyst for Knoevenagel condensation reaction at optimum conditions

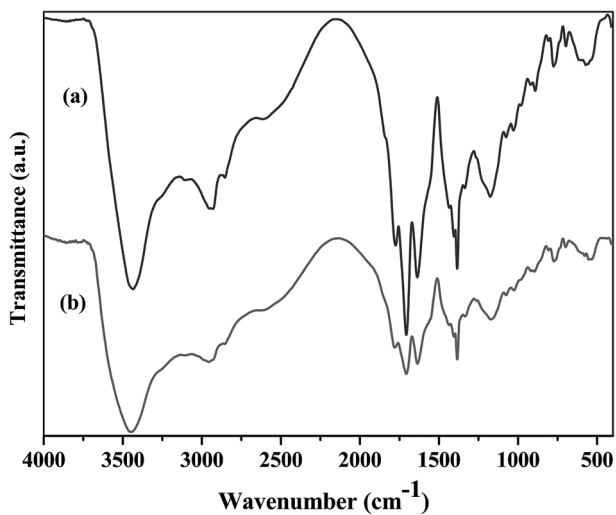


Fig. 11 FT-IR spectra of BPEI-CDs before and after Knoevenagel reaction

Table 2 Comparison of present work (catalyst BPEI-capped CDs) with other studies in the literature

Entry	Catalysts	Reaction conditions: Amount of catalysts, Solvent, Temperature, Time	Conversion (selectivity)%	Ref
1	BPEI-capped CDs	25 mg, EtOH, 60 °C, 2 h	100 (100)	This work
2	(HDTMAp)-[Si]-MCM-41 ^a	100 mg, Benzene, RT, 6 h	94 (100)	[27]
3	AAPTMS@K10 ^b	50 mg, Solvent free, RT, 12 h	99 (99)	[29]
4	Fe ₃ O ₄ @SiO ₂ @NH-NH ₂ -PW ^c	40 mg, EtOH, RT, 18 h 40 mg, EtOH, Reflux, 2 h	90 (-) 80 (-)	[39]
5	Fe ₃ O ₄ /Betti base ^d	50 mg, EtOH, 25 °C, 1.2 h	95 (-)	[40]
6	N-GO ^e	100 mg, CH ₃ CN, 40 °C, 4 h	96.5 (97.3)	[41]
7	CN-Mic ^f	100 mg, CH ₃ CN, 90 °C, 4 h	87.1 (97.1)	[42]
8	Zeolite Imidazolate Framework ZIF-8	20 mg, Toluene, RT, 6 h	100 (-)	[32]
9	UiO-66-NH ₂	60 mg, MeOH, 40 °C, 1 h	95 (-)	[30]
10	UiO-66-NH ₂	144 mg, DMF, 40 °C, 40 min	98 (100)	[31]
11	Zeolite Imidazolate Framework ZIF-9	28 mg, Toluene, RT, 6 h	49 (-)	[33]
12	Znβ (Zn exchanged β zeolites)	100 mg, Solvent free, 140 °C, 6 h	16.1 (-)	[26]
13	Cu-BTC	200 mg, Xylene, 80 °C, 0.5 h	100 (100)	[43]
14	Fe-BTC	200 mg, Xylene, 130 °C, 3 h	100 (99)	[43]

^aSOCMs: Silicate–organic composite materials

^bAAPTMS: N-(2-amino ethyl)-3-amino propyl trimethoxysilane

^cMagnetite-polyoxometalate hybrid nanomaterial was prepared by grafting of H₃PW₁₂O₄₀ on the diamine-functionalized Fe₃O₄ magnetite nanoparticles

^dFe₃O₄ magnetic nanoparticles coated by (3-aminopropyl)triethoxysilane with β-naphthol and benzaldehyde

^eN-GO by grafting of ethylenediamine on the surface of GO

^fCN-Mic: Microporous graphitic carbon nitride material

Finally, in order to compare our results with those reported in literature, Table 2 was included. The preparation of BPEI-CDs as a new Knoevenagel heterogeneous catalyst in one step in a free metal procedure together with low reaction time, and high conversion and selectivity are some advantages of this work.

Conclusion

In this work modified Carbon dots with citric acid and branched polyethylenimine (BPEI) was prepared and designated as BPEI-CDs. The prepared BPEI-CDs was characterized using with a variety of different techniques, including FT-IR, XRD, HRTEM and AFM. The BPEI-CDs was used as basic catalyst for Knoevenagel reactions with aromatic aldehydes and malononitrile. It was found that the unsubstituted aldehyde and substituted with electron-withdrawing groups are more active than those containing electron-releasing groups. It was also found that the

catalyst can be easily recovered from reaction mixtures and reused at least three times without significant loss in catalytic activity.

Acknowledgements The authors would appreciate of Alzahra University for financial support.

Compliance with ethical Standards

Conflict of interest On behalf of all authors, the corresponding author states that there is no conflict of interest.

References

1. Georgakilas V, Perman JA, Tucek J, Zboril R (2015) Broad family of carbon nanoallotropes: classification, chemistry, and applications of fullerenes, carbon dots, nanotubes, graphene, nanodiamonds, and combined superstructures. *Chem Rev* 115(11):4744–4822. <https://doi.org/10.1021/cr500304f>
2. Sun Y-P, Zhou B, Lin Y, Wang W, Fernando KS, Pathak P, Mezzani MJ, Harruff BA, Wang X, Wang H (2006) Quantum-sized carbon dots for bright and colorful photoluminescence. *J Am Chem Soc* 128(24):7756–7757. <https://doi.org/10.1021/ja062677d>
3. Wang Y, Hu A (2014) Carbon quantum dots: synthesis, properties and applications. *J Mat Chem C* 2(34):6921–6939. <https://doi.org/10.1039/C4TC00988F>
4. Li H, Kang Z, Liu Y, Lee S-T (2012) Carbon nanodots: synthesis, properties and applications. *J mat chem* 22(46):24230–24253. <https://doi.org/10.1039/C2JM34690G>
5. Qiao Z-A, Wang Y, Gao Y, Li H, Dai T, Liu Y, Huo Q (2010) Commercially activated carbon as the source for producing multicolor photoluminescent carbon dots by chemical oxidation. *Chem Commun* 46(46):8812–8814. <https://doi.org/10.1039/C0CC02724C>
6. Dong Y, Zhou N, Lin X, Lin J, Chi Y, Chen G (2010) Extraction of electrochemiluminescent oxidized carbon quantum dots from activated carbon. *Chem Mat* 22(21):5895–5899. <https://doi.org/10.1021/cm101884a>
7. Shen L, Zhang L, Chen M, Chen X, Wang J (2013) The production of pH-sensitive photoluminescent carbon nanoparticles by the carbonization of polyethylenimine and their use for bioimaging. *Carbon* 55:343–349. <https://doi.org/10.1016/j.carbon.2012.12.074>
8. Zhou J, Booker C, Li R, Zhou X, Sham T-K, Sun X, Ding Z (2007) An electrochemical avenue to blue luminescent nanocrystals from multiwalled carbon nanotubes (MWCNTs). *J Am Chem Soc* 129(4):744–745. <https://doi.org/10.1021/ja0669070>
9. Shinde DB, Pillai VK (2012) Electrochemical preparation of luminescent graphene quantum dots from multiwalled carbon nanotubes. *Chemistry A* 18(39):12522–12528. <https://doi.org/10.1002/chem.201201043>
10. Zheng L, Chi Y, Dong Y, Lin J, Wang B (2009) Electrochemiluminescence of water-soluble carbon nanocrystals released electrochemically from graphite. *J Am Chem Soc* 131(13):4564–4565. <https://doi.org/10.1021/ja809073f>
11. Zhao Q-L, Zhang Z-L, Huang B-H, Peng J, Zhang M, Pang D-W (2008) Facile preparation of low cytotoxicity fluorescent carbon nanocrystals by electrooxidation of graphite. *Chem Commun* 41:5116–5118. <https://doi.org/10.1039/b812420e>
12. Yang S-T, Cao L, Luo PG, Lu F, Wang X, Wang H, Mezzani MJ, Liu Y, Qi G, Sun Y-P (2009) Carbon dots for optical imaging in vivo. *J Am Chem Soc* 131(32):11308–11309. <https://doi.org/10.1021/ja904843x>
13. Zhai X, Zhang P, Liu C, Bai T, Li W, Dai L, Liu W (2012) Highly luminescent carbon nanodots by microwave-assisted pyrolysis. *Chem Commun* 48(64):7955–7957. <https://doi.org/10.1039/C2CC33869F>
14. Titirici M-M, Antonietti M (2010) Chemistry and materials options of sustainable carbon materials made by hydrothermal carbonization. *Chem Soc Rev* 39(1):103–116. <https://doi.org/10.1039/B819318P>

15. Zhang Y-Q, Ma D-K, Zhuang Y, Zhang X, Chen W, Hong L-L, Yan Q-X, Yu K, Huang S-M (2012) One-pot synthesis of N-doped carbon dots with tunable luminescence properties. *J Mat Chem* 22(33):16714–16718. <https://doi.org/10.1039/C2JM32973E>
16. Dong Y, Wang R, Li H, Shao J, Chi Y, Lin X, Chen G (2012) Polyamine-functionalized carbon quantum dots for chemical sensing. *Carbon* 50(8):2810–2815. <https://doi.org/10.1016/j.carbon.2012.02.046>
17. Lai C-W, Hsiao Y-H, Peng Y-K, Chou P-T (2012) Facile synthesis of highly emissive carbon dots from pyrolysis of glycerol; gram scale production of carbon dots/mSiO₂ for cell imaging and drug release. *J Mat Chem* 22(29):14403–14409. <https://doi.org/10.1039/C2JM32206D>
18. Ma Z, Ming H, Huang H, Liu Y, Kang Z (2012) One-step ultrasonic synthesis of fluorescent N-doped carbon dots from glucose and their visible-light sensitive photocatalytic ability. *New J Chem* 36(4):861–864. <https://doi.org/10.1039/C2NJ20942J>
19. Bigi F, Chesini L, Maggi R, Sartori G (1999) Montmorillonite KSF as an inorganic, water stable, and reusable catalyst for the Knoevenagel synthesis of coumarin-3-carboxylic acids. *J Org Chem* 64(3):1033–1035. <https://doi.org/10.1021/jo981794r>
20. Yu N, Aramini JM, Germann MW, Huang Z (2000) Reactions of salicylaldehydes with alkyl cyanoacetates on the surface of solid catalysts: syntheses of 4H-chromene derivatives. *Tetrahedron Lett* 41(36):6993–6996. [https://doi.org/10.1016/S0040-4039\(00\)01195-3](https://doi.org/10.1016/S0040-4039(00)01195-3)
21. Liang F, Pu Y-J, Kurata T, Kido J, Nishide H (2005) Synthesis and electroluminescent property of poly (p-phenylenevinylene) s bearing triarylamine pendants. *Polymer* 46(11):3767–3775. <https://doi.org/10.1016/j.polymer.2005.03.036>
22. Texier-Boullet F, Foucaud A (1982) Knoevenagel condensation catalysed by aluminium oxide. *Tetrahedron Lett* 23(47):4927–4928. [https://doi.org/10.1016/S0040-4039\(00\)85749-4](https://doi.org/10.1016/S0040-4039(00)85749-4)
23. Rao PS, Venkataratnam R (1991) Zinc chloride as a new catalyst for Knoevenagel condensation. *Tetrahedron Lett* 32(41):5821–5822. [https://doi.org/10.1016/S0040-4039\(00\)93564-0](https://doi.org/10.1016/S0040-4039(00)93564-0)
24. Bartoli G, Bosco M, Carlone A, Dalpozzo R, Galzerano P, Melchiorre P, Sambri L (2008) Magnesium perchlorate as efficient lewis acid for the Knoevenagel condensation between β -diketones and aldehydes. *Tetrahedron Lett* 49(16):2555–2557. <https://doi.org/10.1016/j.tetlet.2008.02.093>
25. Climent MJ, Corma A, Domínguez I, Iborra S, Sabater MJ, Sastre G (2007) Gem-diamines as highly active organocatalysts for carbon–carbon bond formation. *J Catal* 246(1):136–146. <https://doi.org/10.1016/j.jcat.2006.11.029>
26. Saravanamurugan S, Palanichamy M, Hartmann M, Murugesan V (2006) Knoevenagel condensation over β and Y zeolites in liquid phase under solvent free conditions. *Appl Catal A* 298:8–15. <https://doi.org/10.1016/j.apcata.2005.09.014>
27. Kubota Y, Nishizaki Y, Ikeya H, Saeki M, Hida T, Kawazu S, Yoshida M, Fujii H, Sugi Y (2004) Organic–silicate hybrid catalysts based on various defined structures for Knoevenagel condensation. *Microporous Mesoporous Mater* 70(1–3):135–149. <https://doi.org/10.1016/j.micromeso.2004.02.017>
28. Mukhopadhyay C, Ray S (2011) A new silica based substituted piperidine derivative catalyzed expeditious room temperature synthesis of homo and hetero bis-Knoevenagel condensation products. *Catal Commun* 12(15):1496–1502. <https://doi.org/10.1016/j.catcom.2011.05.033>
29. Varadwaj GBB, Rana S, Parida K (2013) Amine functionalized K10 montmorillonite: a solid acid–base catalyst for the Knoevenagel condensation reaction. *Dalton Trans* 42(14):5122–5129. <https://doi.org/10.1039/c3dt32495h>
30. Panchenko VN, Matrosova MM, Jeon J, Jun JW, Timofeeva MN, Jung SH (2014) Catalytic behavior of metal–organic frameworks in the Knoevenagel condensation reaction. *J Catal* 316:251–259. <https://doi.org/10.1016/j.jcat.2014.05.018>
31. Yang Y, Yao H-F, Xi F-G, Gao E-Q (2014) Amino-functionalized Zr (IV) metal–organic framework as bifunctional acid–base catalyst for Knoevenagel condensation. *J Mol Catal A* 390:198–205. <https://doi.org/10.1016/j.molcata.2014.04.002>
32. Tran UP, Le KK, Phan NT (2011) Expanding applications of metal–organic frameworks: zeolite imidazolate framework ZIF-8 as an efficient heterogeneous catalyst for the Knoevenagel reaction. *ACS Catal* 1(2):120–127. <https://doi.org/10.1021/cs1000625>
33. Nguyen LT, Le KK, Truong HX, Phan NT (2012) Metal–organic frameworks for catalysis: the Knoevenagel reaction using zeolite imidazolate framework ZIF-9 as an efficient heterogeneous catalyst. *Catal Sci Technol* 2(3):521–528. <https://doi.org/10.1039/c1cy00386k>

34. Xamena FL, Cirujano F, Corma A (2012) An unexpected bifunctional acid base catalysis in IRMOF-3 for Knoevenagel condensation reactions. *Microporous Mesoporous Mater* 157:112–117. <https://doi.org/10.1016/j.micromeso.2011.12.058>
35. Farzaneh F, Maleki MK, Rashtizadeh E (2017) Expedient catalytic access to Knoevenagel condensation using Sr₃Al₂O₆ nanocomposite in room temperature. *J Clust Sci* 28(6):3253–3263. <https://doi.org/10.1007/s10876-017-1288-8>
36. Wu P, Li W, Wu Q, Liu Y, Liu S (2017) Hydrothermal synthesis of nitrogen-doped carbon quantum dots from microcrystalline cellulose for the detection of Fe³⁺ ions in an acidic environment. *RSC Adv* 7(70):44144–44153. <https://doi.org/10.1039/C7RA08400E>
37. Gascon J, Aktay U, Hernandez-Alonso MD, van Klink GP, Kapteijn F (2009) Amino-based metal-organic frameworks as stable, highly active basic catalysts. *J Catal* 261(1):75–87. <https://doi.org/10.1016/j.jcat.2008.11.010>
38. Corma A, Iborra S, Rodriguez I, Sanchez F (2002) Immobilized proton sponge on inorganic carriers: the synergic effect of the support on catalytic activity. *J catal* 211(1):208–215. <https://doi.org/10.1006/jcat.2002.3692>
39. Shahbazi F, Amani K (2014) Synthesis, characterization and heterogeneous catalytic activity of diamine-modified silica-coated magnetite-polyoxometalate nanoparticles as a novel magnetically-recoverable nanocatalyst. *Catal Commun* 55:57–64. <https://doi.org/10.1016/j.catcom.2014.06.006>
40. Heidari P, Cheraghali R, Veisi H (2016) Betti base-modified magnetic nanoparticles as a novel basic nanocatalyst in Knoevenagel condensation and its related palladium nanocatalyst in Suzuki coupling reactions. *Appl Organomet Chem* 30(12):991–997. <https://doi.org/10.1002/aoc.3532>
41. Xue B, Zhu J, Liu N, Li Y (2015) Facile functionalization of graphene oxide with ethylenediamine as a solid base catalyst for Knoevenagel condensation reaction. *Catal Commun* 64:105–109. <https://doi.org/10.1016/j.catcom.2015.02.003>
42. Xu J, Shen K, Xue B, Li Y-X (2013) Microporous carbon nitride as an effective solid base catalyst for Knoevenagel condensation reactions. *J Mol Catal A-Chem* 372:105–113. <https://doi.org/10.1016/j.molcata.2013.02.019>
43. Opanasenko M, Dhakshinamoorthy A, Shamzhy M, Nachtigall P, Horáček M, Garcia H, Čejka J (2013) Comparison of the catalytic activity of MOFs and zeolites in Knoevenagel condensation. *Catal Sci Technol* 3(2):500–507. <https://doi.org/10.1039/C2CY20586F>

Publisher's Note Springer Nature remains neutral with regard to jurisdictional claims in published maps and institutional affiliations.